

Experimental observation of real spectra in Parity-Time symmetric ZRC dimers with positive and negative frequencies

Stéphane Boris Tabeu^{1,2,3,*}, Fernande Fotsa-Ngaffo⁴, Senghor Tagouegni^{1,2}, Kazuhiro Shouno⁵, and Aurélien Kenfack-Jiotsa^{2,6}
1 Laboratory of Mechanics, Materials and Structures, Department of Physics, Faculty of Science, University of Yaounde I, P.O. Box 812, Yaounde, Cameroon

2 Nonlinear Physics and Complex Systems Group, Department of Physics, The Higher Teacher's Training College, University of Yaounde I, P.O. Box 47, Yaounde, Cameroon

3 Laboratory of Electronics and Signal Processing, Department of Electrical and Telecommunication Engineering, National Advanced School of Engineering, University of Yaounde I, P.O. Box 8390, Yaounde, Cameroon

4 Institute of Wood technologies, University of Yaounde I, P.O. Box 306, Mbalmayo, Cameroon

5 Graduate School of Systems and Information Engineering, University of Tsukuba, Ibaraki 305-8573, Japan and

6 High-Tech and Slow Technology (HITASTE), P.O. Box 105, Yaounde, Cameroon

(Dated: November 11, 2021)

We present in this work the first experimental observation of oscillations in Parity-Time symmetric ZRC dimers. The system obtained is of first order ordinary differential equation due to the use of imaginary resistors. The coupled cells must share the same type of frequency: positive or negative. We observed the real and imaginary parts of the voltage across the components of a ZRC cell. Exceptional points are well identified. This work may be very useful in the generation of new type of oscillators. It can also be used in the design of new optoelectronic devices for major applications in the transport of information and the mimics of two-level systems for quantum computing.

Keywords: Non-Hermitian systems, Parity-time symmetry, Imaginary resistor, ZRC-Dimer, Negative frequency

I. INTRODUCTION

Non-Hermitian systems are today a major fields of investigations in different specialities. In 1998, Carl Bender demonstrated that a non-Hermitian systems can have a real spectra without being Hermitian opening the road to Parity-Time (PT) Symmetry [1–3]. In Quantum Mechanics, this reality is related to the potential which satisfied $V(x) = V^*(-x)$ with an even real part and odd imaginary part [1–6]. In Optics, the refractive index of the medium must satisfied a relation of the same nature $n(x) = n^*(-x)$ [7–13] and $\varepsilon(x) = \varepsilon^*(-x)$ for dielectric permittivity in Metamaterials [14–17]. The notion of Parity-Time Symmetry is also extended to many order fields such as Photonics [7–13], Mechanics [18–20], Optomechanics [20–23], Acoustics [24–26] and Electronics [27–31] just to name few. In 2010, Reuter realized the first experimental demonstration of PT-symmetry in Optics by coupling two waveguides having equal amount of gain and loss [7]. In 2011, Schindler et al used two active RLC circuits to introduce the notion in Electronics [27, 28]. The loss cell was represented by a natural positive resistor and the gain cell by a negative resistor using Negative impedance con-

verter. In 2013, the team of Carl Bender experimentally demonstrate the real spectra in coupled mechanic oscillators [18]. The Rabi oscillations occurred near the the exceptional point in the response of the system. More after it was presented the counterpart of Parity-Time symmetry: The Anti-Parity Time symmetry. In this new Physics, the loss and the gain are exclusively in the dimers [30, 32–38]. In Quantum Mechanics, the potential follows the relation $V(x) = -V^*(-x)$, the refractive index $n(x) = -n^*(-x)$ in Optics and $\varepsilon(x) = -\varepsilon^*(-x)$ for the dielectric permittivity in Metamaterials. Now the real parts of the potential, the refractive index of the medium and the permittivity are odd and their imaginary parts even giving rise to the coupled of Gain-Gain cells or Loss-Loss cells to made Anti-Parity Time symmetry. In others fields, the rotating frame is used to create indirectly positive and negative frequencies in the cells of the dimer such as in lasers gyroscopes [36]. It also used the Coupled Mode Theory (CMT) and adiabatic elimination in optical waveguides, slowly varying envelope approximation in Nanophotonics to achieve the same reality. Many others works are also presented in these directions [30–37]. Tabeu et al presented in [30] how to achieve Parity-Time symmetry and Anti-Parity time symmetry in electronics using imaginary resistors [31, 39, 40] to have directly the system of first order ordinary differential equation without the coupling mode theory or

* Correspondence email address: stephaneboris@yahoo.fr

the rotating frame. The configurations presented were with Gain-Loss, Gain-Gain and Loss-Loss in the dimer. All these (Anti)-Parity-time systems have many applications such as sensing and telemetry, non-reciprocal transport of information, generation of qubits for quantum computing, wireless power transfer, switches, single mode power Lasers [9–12, 17, 30, 31, 34, 38, 40–46] and others .

In this works, we proposed the experimental realization of ZRC cells and a PT-dimer based imaginary resistors. Since the Hamiltonian of the resulted system is the same which the one encounter after some transformations in Optics and Photonics, it can mimics easily such these systems and gather the bridge for new devices in Optoelectronics and Photoelectronics with the avenue of optical and photonic quantum computing. The paper is organized as follows: In Sect. II the RLC and ZRC are presented with their frequencies. In Sect. III, the ZRC PT-dimer is studied. Its eigenvalues are calculated and some simulations of its dynamic behavior are driven. In Sect. IV, the experimental realization of the dimer is presented and the oscillations across the gain and loss cells. The paper end with a conclusion.

II. RLC AND ZRC CELLS

A. Real volatge in RLC circuit

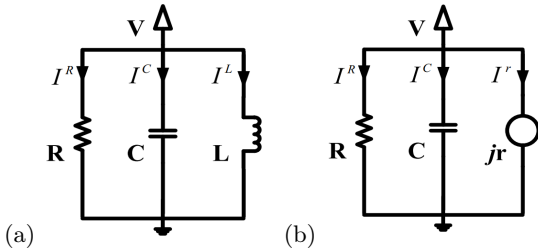


Figure 1: (a) The RLC cell is constituted of a real resistor R , an inductor L and a capacitor C . All the components are mounted in parallel. The ZRC cell is constituted of an imaginary resistor $Z = jr$, a real resistor R and a capacitor C all mounted in parallel.

The RLC cell contains a real resistor, a capacitor and an inductor Fig.1(a) The Kirchoff's law applied at the node gives us:

$$I^R + I^L + I^C = 0 \quad (1)$$

By applying the Ohm's law at the borders of the components, we have a second order form of ordinary differential equation depicted as :

$$\frac{d^2V}{dt^2} + \gamma \frac{dV}{dt} + \omega_0^2 V = 0 \quad (2)$$

With $\gamma = \frac{1}{RC}$ representing the damping rate and $\omega_0 = \sqrt{\frac{1}{LC}}$ the natural frequency of the cell. We look a solution in the form $V \propto e^{j\alpha t}$ and it derives from Eq. (2) a second order equation in α :

$$\alpha^2 - j\gamma - \omega_0^2 = 0 \quad (3)$$

The final voltage with an appropriate choice of initial conditions is :

$$V(t) = \frac{1}{2} V_0 e^{-(\frac{\gamma}{2})t} (e^{j\omega t} + e^{-j\omega t}) \quad (4)$$

$$\alpha_{1,2} = j \left(\frac{\gamma}{2} \right) \pm \sqrt{\omega_0^2 - \left(\frac{\gamma}{2} \right)^2} = 0 \quad (5)$$

with $\omega = \sqrt{\omega_0^2 - \left(\frac{\gamma}{2} \right)^2}$.

The system is under-damped if $\omega > 0$. Then, the system is pseudo-oscillatory with exactly the combination of two voltages with positive and negative frequencies:

$$V(t) = \mathbf{V}(\omega) + \mathbf{V}(-\omega) \quad (6)$$

The result is exactly a real value.

$$V(t) = V_0 e^{-(\frac{\gamma}{2})t} \cos(\omega t) \quad (7)$$

B. Complex voltage in ZRC circuit

The imaginary resistor is a resistor which resistance is a pure imaginary number. It is built indirectly by gyrators [39]. If it is associated to a resistor which resistance is a real number, we can have a complex resistor which impedance is in the form $R_C = R + jr = |R_C| e^{j\Phi}$. R represents the real part and r the imaginary part ($|R_C| = \sqrt{R^2 + r^2}$; $\tan(\Phi) = \frac{r}{R}$). The ZRC cell is constituted by a capacitor C , a real resistor R and at least an imaginary resistor $Z = jr$ [30, 31]. The value of components may be positive or negative without any restrictions. The cell is depicted in Fig. 1(b). The Kirchoff's law applied at the node gives us:

$$I^Z + I^R + I^C = 0 \quad (8)$$

The Ohm's law at the borders of resistors involves:

$$V = RI^R = ZI^Z \quad (9)$$

From the combination of Eq. 8 and Eq. 9, we deduce the following:

$$C \frac{dV}{dt} + \frac{V}{R} - j \frac{V}{r} = 0 \quad (10)$$

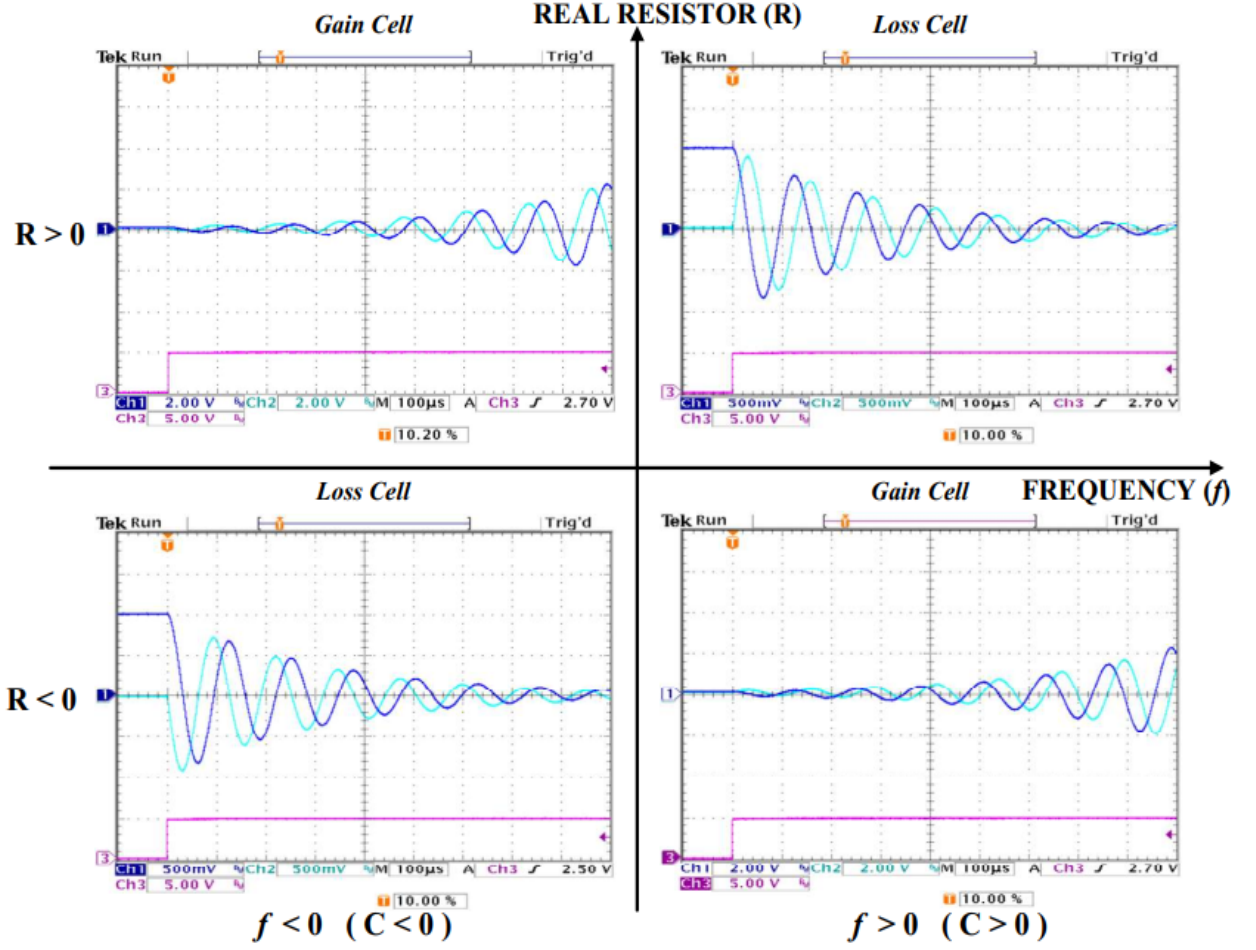


Figure 2: Experimental realization of ZRC circuits with positive and negative frequencies. Pseudo-oscillations of the real $\text{Re}(\mathbf{V}(\omega)) = V_0 e^{-\gamma t} \cos(\omega t)$ (in blue) and the imaginary $\text{Im}(\mathbf{V}(\omega)) = V_0 e^{-\gamma t} \sin(\omega t)$ (in cyan) parts of the voltage. The sign of the frequency is the one of the capacitors. The experiments run a $f \approx \pm 7.96 \text{ kHz}$. The others values of components are: $Z = j2k\Omega$ for the imaginary resistor; $R = \pm 30 \text{ k}\Omega$ for the real resistors and $C = \pm 10 \text{ nF}$ for capacitors

$$\frac{dV}{dt} + \left(\frac{1}{RC} - j \frac{1}{rC} \right) V = 0 \quad (11)$$

The final voltage with an appropriate initial conditions is:

$$V(t) = V_0 e^{(-\frac{1}{RC}t)} e^{(j\frac{1}{rC}t)} \quad (12)$$

We obtained a complex voltage across the components of the circuit given as:

$$V(t) = V_0 e^{(-\gamma t)} e^{(j\omega t)} = V_0 e^{(-\gamma t)} (\cos(\omega t) + j \sin(\omega t)) \quad (13)$$

with $\gamma = \frac{1}{RC}$ and $\omega = \frac{1}{rC}$ which may be positive or negative.

The system with positive frequency does not describe

the same reality with the one with negative frequency because $\cos(\omega t)$ is even and $\sin(\omega t)$ is odd.

$$\begin{cases} \mathbf{V}(\omega) = V_0 e^{(-\gamma t)} (\cos(\omega t) + j \sin(\omega t)) \\ \mathbf{V}(-\omega) = V_0 e^{(-\gamma t)} (\cos(\omega t) - j \sin(\omega t)) \end{cases} \quad (14)$$

$$\begin{cases} \text{Re}(\mathbf{V}(\omega)) = \text{Re}(\mathbf{V}(-\omega)) = V_0 e^{(-\gamma t)} \cos(\omega t) \\ \text{Im}(\mathbf{V}(\omega)) = -\text{Im}(\mathbf{V}(-\omega)) = V_0 e^{(-\gamma t)} \sin(\omega t) \end{cases} \quad (15)$$

Since this response of the system is complex, based on the model of the imaginary resistor proposed in Ref.[39], one can probe the real part $\text{Re}(\mathbf{V}(\omega)) = V_0 e^{(-\gamma t)} \cos(\omega t)$ and the imaginary part $\text{Im}(\mathbf{V}(\omega)) = V_0 e^{(-\gamma t)} \sin(\omega t)$ of the system simultaneously. The sign of the damping rate define the nature of the cell. Depending on the signs of the components, When $\gamma < 0$,

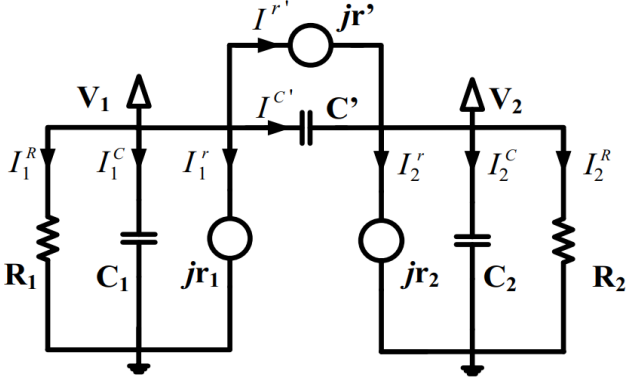


Figure 3: The circuit of the ZRC Dimer. Each cell contains in parallel an imaginary resistor $Z_n = jr_n$, a real resistor R_n , a capacitor C_n . The ZRC-cells are coupled by an imaginary resistor $z = jr'$ or a capacitor C' or by all of them.

we have a gain cell and when $\gamma > 0$, we have a loss cell. The experimental verification of the behavior of the cell with positive and negative frequencies is given in Fig. 2. The real and the imaginary parts of the voltage are presented simultaneously for each case. The sign of the frequency is the one of the capacitor in the cell. This gives the possibilities to achieve experimentally PT-symmetric systems with cells of same frequency and Anti-Parity-Time (APT) symmetry with cells of opposite frequencies without the rotating frame condition as in existing systems in others fields of Physics. These results open new avenues for experimental non-Hermitian Quantum Mechanics and Quaternionic Quantum Electronics.

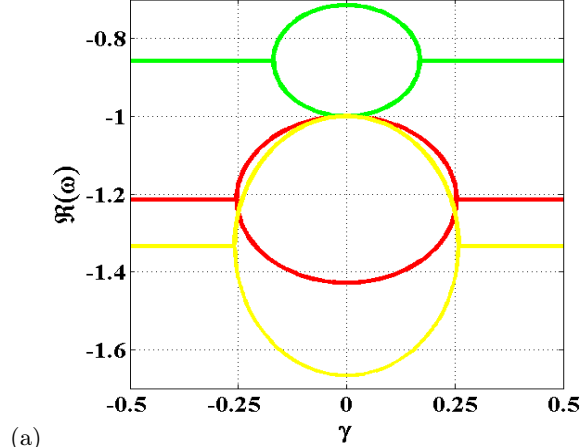
III. ZRC PARITY-TIME SYMMETRIC DIMER

A. The ZRC model and equations of dynamics

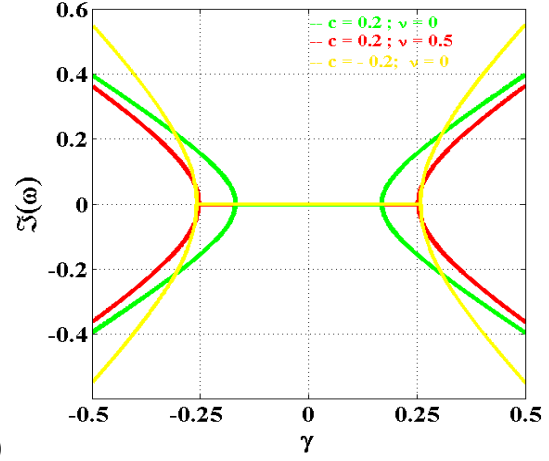
The ZRC PT- symmetric dimer is made by two active ZRC-cells. The cells contain in parallel an imaginary resistor, a capacitor and a real resistor. They are coupled by a capacitor or an imaginary resistor or by all of them. The values of components may be positive or not without any restriction. In Fig. 3 is presented the setup of the ZRC PT-symmetric dimer. By applying the Kirchoff's laws at nodes 1 and 2, we have:

$$\begin{cases} I_1^R + I_1^C + I_1^Z + I_1^G + I^{C'} + I^{r'} = 0 \\ I_2^R + I_2^C + I_2^Z + I_2^G - I^{C'} - I^{r'} = 0 \end{cases} \quad (16)$$

with $I_n^C = C_n \frac{d}{dt} V_n$; $I^{C'} = C' \frac{d}{dt} (V_0 - V_1)$; $I_n^R = \frac{V_n}{R_n}$; $I_n^Z = -j \frac{V_n}{r_n}$; $I^{r'} = \frac{1}{R'} (V_1 - V_2)$; $I^{r'} = -j \frac{1}{r'} (V_1 - V_2)$



(a)



(b)

Figure 4: The eigenvalues of the setup corresponding to three cases in which we have a positive and negative capacitive couplings and at last a case with both the capacitive and the imaginary couplings. (a) Real parts of the eigenvalues (b) Imaginary parts of the eigenvalues

for all the components. These considerations lead on the general form of first order ordinary differential equations:

$$\begin{cases} \frac{dV_1}{d\tau} = \frac{1}{\Delta} [(1 + c_2) (j(1 + \nu_1) - \gamma_1) - jc_1 \Gamma \nu_2] V_1 \\ + \frac{1}{\Delta} [-j(1 + c_2) \nu_1 + c_1 \Gamma (j(1 + \nu_2) - \gamma_2)] V_2 \\ \frac{dV_2}{d\tau} = \frac{1}{\Delta} [-j(1 + c_1) \Gamma \nu_2 + c_2 (j(1 + \nu_1) - \gamma_1)] V_1 \\ + \frac{1}{\Delta} [(1 + c_1) \Gamma (j(1 + \nu_2) - \gamma_2) - jc_2 \nu_1] V_2 \end{cases} \quad (17)$$

where $\tau = \omega_1 t$; $\omega_n = \frac{1}{r_n C_n}$; $\Gamma = \frac{\omega_2}{\omega_1}$; $c_n = \frac{C'}{C_n}$; $\nu_n = \frac{r_n}{r'}$; $\gamma_n = \frac{r_n}{R_n}$ and $\Delta = 1 + \sum_{n=1}^2 c_n$.

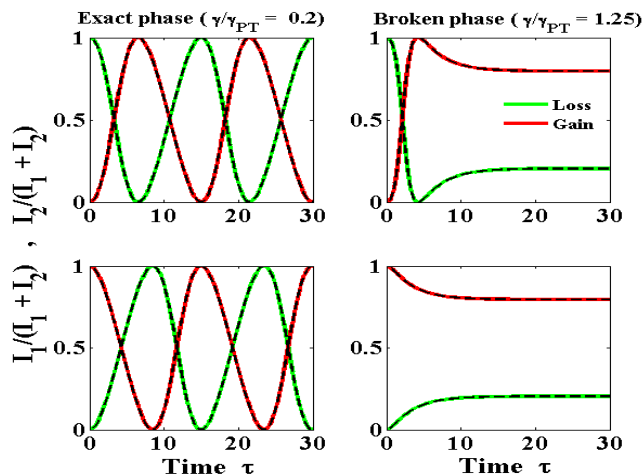


Figure 5: Relative values of the modules of complex voltages across the gain and loss cells $I_n = |V_n(\tau)|^2$ with different initial inputs. In the exact phase, there are normal oscillations with an amplification of the initial input due the presence of gain and loss in the setup. In the broken phase, there is an exponential growth and also a deep difference between the behavior of gain and loss cells

The system of first order ordinary differential equation is PT- symmetric when the several conditions are satisfied:

$$\begin{cases} \Gamma = 1; c_1 = c_2 = c \\ \nu_1 = \nu_2 = \nu; \gamma_1 = -\gamma_2 = \gamma \end{cases} \quad (18)$$

We can associate to our system a non-Hermitian effective Hamiltonian such that :

$$j \frac{d}{d\tau} |\Psi(\tau)\rangle = H_{eff} |\Psi(\tau)\rangle \quad (19)$$

where: j is the imaginary unit ($j^2 = -1$); $|\Psi(\tau)\rangle = (V_1(\tau), V_2(\tau))^T$; $H_{eff} = k_0 I + k_x \sigma_x + k_y \sigma_y + k_z \sigma_z$. I is the 2×2 matrix unit and σ_x , σ_y and σ_z are Pauli's matrices.

$$\sigma_x = \begin{pmatrix} 0 & 1 \\ 1 & 0 \end{pmatrix}; \sigma_y = \begin{pmatrix} 0 & -j \\ j & 0 \end{pmatrix}; \sigma_z = \begin{pmatrix} 1 & 0 \\ 0 & -1 \end{pmatrix} \quad (20)$$

The complex coefficients k_0, k_x, k_y , and k_z are function of the independent real parameters of the system deduced as :

$$\begin{cases} k_0 = -(1 + c + \nu)/\Delta; k_x = -(c - \nu)/\Delta \\ k_y = -c\gamma/\Delta; k_z = -j(1 + c)\gamma/\Delta \end{cases} \quad (21)$$

Since the system is PT-symmetric, it satisfied the following relation:

$$[\mathbf{PT}, H_{eff}] = 0 \quad (22)$$

where $\mathbf{P} = \sigma_x$ is the Parity operator and $\mathbf{T} = K$ is the time reversal operator with K being the complex conjugation operation. That is k_0, k_x and k_y must be real whereas k_z must be purely imaginary. The eigenvalues of the Hamiltonian resulted from $\det(H_{eff} - \omega I) = 0$ are given as follow:

$$\omega_{\pm} = k_0 \pm \sqrt{k_x^2 + k_y^2 + k_z^2} \quad (23)$$

B. The eigenvalues of the ZRC PT-dimer and oscillations

Function of the real parameters of the system, the eigenvalues of the effective Hamiltonian are :

$$\omega_{\pm} = \frac{-(1 + c + \nu) \pm \sqrt{(1 + 2c)(\gamma_{PT}^2 - \gamma^2)}}{1 + 2c} \quad (24)$$

with $\gamma_{PT} = \pm \frac{|c - \nu|}{\sqrt{1 + 2c}}$.

The system is PT-unbreakable if $c < -1/2$ and PT-breakable $c > -1/2$. When $c = \nu$, one have a non-Hermitian diabolic point in the unbreakable Parity-Time symmetry and a thresholdless point in the breakable Parity-Time symmetry.

The exceptional points are where both eigenvalues and eigenvectors coalesce. There are well identified in Fig. 4. Three cases are presented. In the first case only the positive capacitive coupling is activated ($c = 0.2; \nu = 0$). When $\gamma < \gamma_{PT}$, all the eigenfrequencies are real ($\text{Re}(\omega_{\pm}) \neq 0; \text{Im}(\omega_{\pm}) = 0$) and we are in the exact phase of Parity-Time Symmetry. When $\gamma = \gamma_{PT}$, the eigenvalues coalesce ($\omega_+ = \omega_-$): this is the exceptional point. Its presence in a system calls for enhancement of sensing than the one with diabolic point, for chiral properties which are revealed when the point is encircled with time varying components in the setup, opening the road to explain the asymmetric transport of information in Optics and in Photonics. It is at this point that happens unidirectional invisibility in the scattering properties of waveguides with Parity-Time symmetry. At last, when $\gamma > \gamma_{PT}$, the real parts of eigenvalues are identical ($\text{Re}(\omega_+) = \text{Re}(\omega_-)$) and the imaginary parts emerge opposite in sign ($\text{Im}(\omega_+) = -\text{Im}(\omega_-)$): we are in the broken phase Parity-Time symmetry. In this phase the system is nonreciprocal and there is a deep difference between gain cell and loss cell when the initial input is set to one or another cell. The Coherent Perfect Absorber-Laser (CPA-L) occurs in the

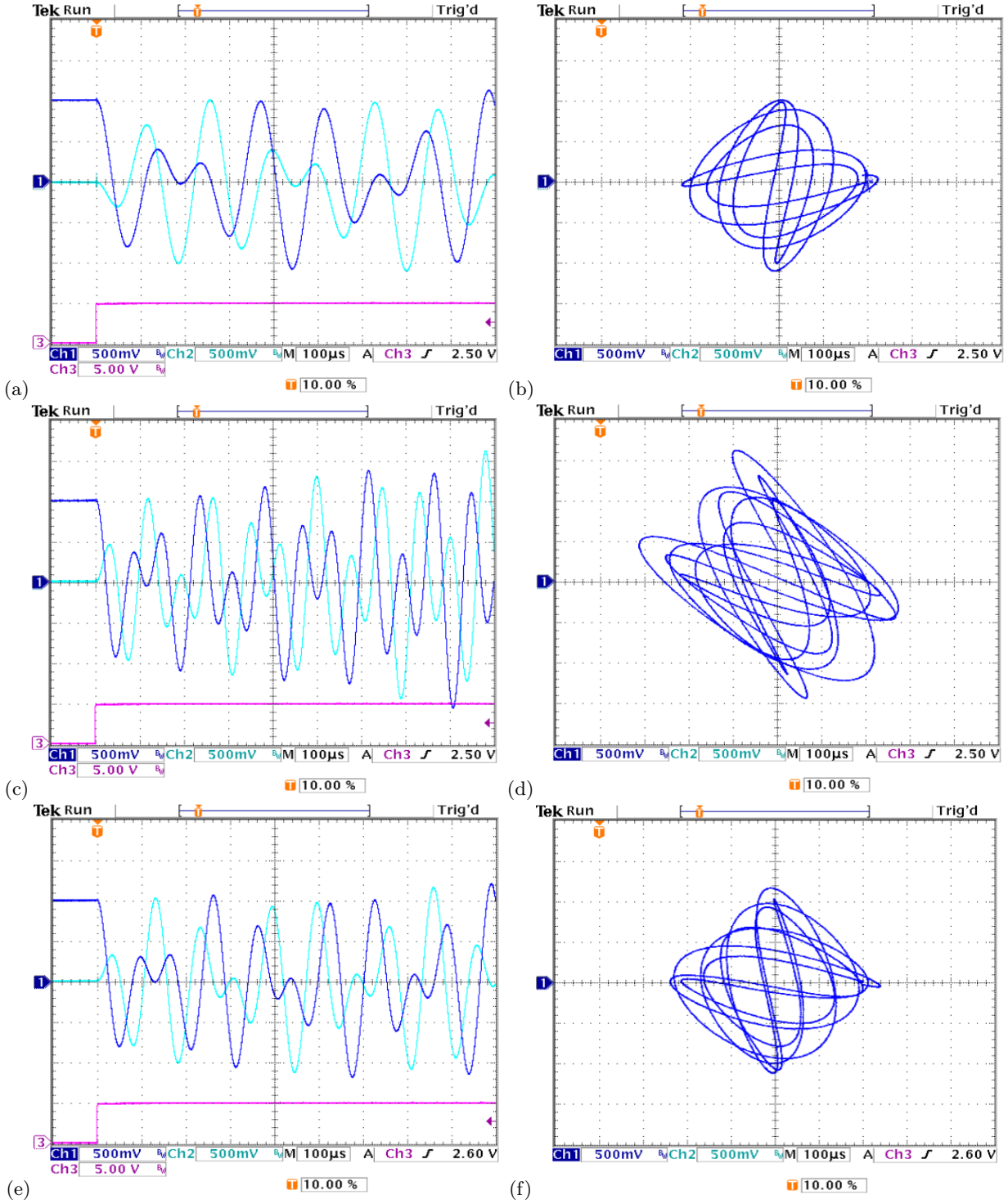


Figure 6: Experimental observation of real part of voltages in the ZRC PT-dimer at $\gamma = 0.2 \gamma_{PT}$. The first case with positive frequency and capacitive coupling $C = 10 \text{ nF}$; $C' = 2 \text{ nF}$; $Z = j2 \text{ k}\Omega$; $c = 0.2$; $\nu = 0$: (a) The real voltage dynamic across the loss and the gain cells ($f \approx 2.23 \text{ kHz}$; $R \approx 59.16 \text{ k}\Omega$) (b) The Lissajous's curve. The second case with negative frequency and capacitive coupling $C = -10 \text{ nF}$; $C' = 2 \text{ nF}$; $Z = j2 \text{ k}\Omega$; $c = -0.2$; $\nu = 0$: (c) The real voltage dynamic across the loss and the gain cells ($f \approx -5.2 \text{ kHz}$; $R \approx 38.73 \text{ k}\Omega$) (d) The Lissajous's curve. The third case with positive frequency, capacitive and imaginary couplings $C = 10 \text{ nF}$; $C' = 2 \text{ nF}$; $Z = j2 \text{ k}\Omega$; $c = 0.2$; $\nu = 0.5$: (e) The real voltage dynamic across the loss and the gain cells ($f \approx 3.34 \text{ kHz}$; $R \approx 39.44 \text{ k}\Omega$) (f) The Lissajous's curve.

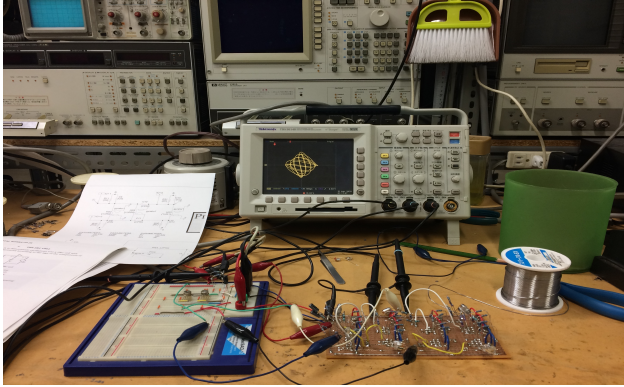


Figure 7: View of the experiment environment

this phase when the scattering properties are investigated in PT-waveguides. We have the same description with the second case with negative capacitive coupling ($c = -0.2$; $\nu = 0$) but more than $-1/2$ to be in the breakable PT-symmetry and the third case with both positive capacitive coupling and imaginary coupling ($c = 0.2$; $\nu = 0.5$). For the third case, analytical solutions and numerical simulations with the algorithm of Runge-Kutta order 4 are presented in Fig. 5. The behaviors of oscillations when the input is set from the loss is equal to the one of the initial input from gain after a beat of time. This confirms the character of non-reciprocity which is a signature of non-Hermitian systems.

IV. EXPERIMENTAL REALIZATION OF OSCILLATIONS IN ZRC PT-DIMER

In this section is presented the experimental realization of the ZRC Parity-Time symmetric dimer with positive and negative frequencies. The imaginary resistor used is in the model of Ref.[39]. One can easily probe the real and imaginary parts of the voltages across the components. We have use the Negative Immitance Converter to achieve negative values of components with resistors, capacitors and operational amplifiers. The realizations are those of the three configurations listed in the previous section at $\gamma = 0.2\gamma_{PT}$. Only the real parts of voltages are presented in Fig. 6. In the first case, the positive natural

frequency of independent cells is $f = 7.96 kHz$. The values of different components are: $Z_0 = Z_1 = Z = j2 k\Omega$; $R_0 = 59.16 k\Omega$ $R_1 = -59.16 k\Omega$; $C_0 = C_1 = C = 10 nF$; $C' = 2 nF$; $jR' = 0$. The frequency of oscillations obtained is $f \approx 2.23 kHz$ (Fig. 6(a-b)). In the second case, the negative natural frequency of independent cells is $f = -7.96 kHz$. The values of different components are: $Z_0 = Z_1 = Z = j2 k\Omega$; $R_0 = 38.73 k\Omega$ $R_1 = -38.73 k\Omega$; $C_0 = C_1 = C = -10 nF$; $C' = 2 nF$; $jR' = 0$. The frequency of oscillations obtained is $f \approx -5.2 kHz$ (Fig. 6(c-d)). In the third case, the positive natural frequency of independent cells is $f = 7.96 kHz$. The values of different components are: $Z_0 = Z_1 = Z = j2 k\Omega$; $R_0 = 39.44 k\Omega$ $R_1 = -39.44 k\Omega$; $C_0 = C_1 = C = 10 nF$; $C' = 2 nF$; $jR' = j4 k\Omega$. The frequency of oscillations obtained is $f \approx 3.34 kHz$ (Fig. 6(e-f)).

Operational amplifiers (LF356), metal-film resistors and polystyrene capacitors are used in the experimental circuits. All the elements are tuned to be within 0.1% with respect to the desired values. For injecting the initial conditions, we have used DG200ABA analog switches and an external standard voltage source. All the waveforms are acquired by Tektronix TDS3014B digital oscilloscope. Agilent 33120A function generator is used to generate the trigger signal for the experimental circuits (See Fig. 7)

V. CONCLUSION

We have reported in this work the experimental realization of the ZRC PT-symmetric Dimer. A comparative study is made between RLC and ZRC cells. Contrary to the RLC cell which dynamic is of second order ordinary differential equation with a real output, the ZRC is of first order ordinary differential equation with a complex output. We succeed the measurements of the real and imaginary parts of the voltage in positive and negative frequencies. Oscillations of the PT-dimers are also probed in the exact phase of the Parity-Time symmetry without any restriction or approximation. This work paves the way for the design of new electronic and optoelectronic devices. It opens the investigation on the exploitation of the new band of negative frequencies in Telecommunications and the generation of new oscillators for simulations of qubits in quantum computing.

[1] C. M. Bender and S. Boettcher, Real Spectra in Non-Hermitian Hamiltonians Having PT-Symmetry, Physical Review Letters, vol. 80, no. 24, pp. 5243-5246, Jun. 1998.

[2] C. M. Bender, S. Boettcher, and P. N. Meisinger, PT-symmetric quantum mechanics, Journal of Mathematical Physics, vol. 40, no. 5, pp. 2201-2229, May 1999.

[3] C. M. Bender, M. V. Berry, and A. Mandilara, Generalized PT symmetry and realspectra, Journal of Physics

- A: Mathematical and General, vol. 35, no. 31, pp. L467-L471, Jul. 2002.
- [4] A. Mostafazadeh, Pseudo-Hermiticity versus PT symmetry: The necessary condition for the reality of the spectrum of a non-Hermitian Hamiltonian, *Journal of Mathematical Physics*, vol. 43, no. 1, pp. 205-214, Jan. 2002
- [5] A. Mostafazadeh and A. Batal, Physical aspects of pseudo-Hermitian and PT-symmetric quantum mechanics, *Journal of Physics A: Mathematical and General*, vol. 37, no. 48, pp. 11645-11679, Nov. 2004.
- [6] A. Mostafazadeh, Application of pseudo-Hermitian quantum mechanics to a PT-symmetric Hamiltonian with a continuum of scattering states, *Journal of Mathematical Physics*, vol. 46, no. 10, p. 102108, Oct. 2005.
- [7] C. E. Rüter, K. G. Makris, R. El-Ganainy, D. N. Christodoulides, M. Segev, and D. Kip, Observation of parity-time symmetry in optics, *Nature Physics*, vol. 6, no. 3, pp. 192-195, Jan. 2010
- [8] S. Nixon and J. Yang, All-real spectra in optical systems with arbitrary gain-and-loss distributions, *Physical Review A*, vol. 93, no. 3, Mar. 2016.
- [9] R. El-Ganainy, K. G. Makris, M. Khajavikhan, Z. H. Musslimani, S. Rotter, and D. N. Christodoulides, Non-Hermitian physics and PT symmetry, *Nature Physics*, vol. 14, no. 1, pp. 11-19, Jan. 2018.
- [10] H. Zhao and L. Feng, Parity-time symmetric photonics, *National Science Review*, vol. 5, no. 2, pp. 183-199, Jan. 2018.
- [11] M.-A. Miri and A. Alù, Exceptional points in optics and photonics, *Science*, vol. 363, no. 6422, p. eaar7709, Jan. 2019.
- [12] K. Özdemir, S. Rotter, F. Nori, and L. Yang, Parity-time symmetry and exceptional points in photonics, *Nature Materials*, vol. 18, no. 8, pp. 783-798, Apr. 2019.
- [13] K. G. Makris, R. El-Ganainy, D. N. Christodoulides, and Z. H. Musslimani, Beam Dynamics in PT-Symmetric Optical Lattices, *Physical Review Letters*, vol. 100, no. 10, Mar. 2008.
- [14] P. Tassin, L. Zhang, T. Koschny, E. N. Economou, and C. M. Soukoulis, Low-Loss Metamaterials Based on Classical Electromagnetically Induced Transparency, *Physical Review Letters*, vol. 102, no. 5, Feb. 2009.
- [15] A. Alù and N. Engheta, All Optical Metamaterial Circuit Board at the Nanoscale, *Physical Review Letters*, vol. 103, no. 14, Sep. 2009.
- [16] H. Alaeian and J. A. Dionne, Parity-time-symmetric plasmonic metamaterials, *Physical Review A*, vol. 89, no. 3, Mar. 2014.
- [17] A. Baev, P. N. Prasad, H. Ågren, M. Samo, and M. Wegener, Metaphotonics: An emerging field with opportunities and challenges, *Physics Reports*, vol. 594, pp. 1-60, Sep. 2015.
- [18] C. M. Bender, B. K. Berntson, D. Parker, and E. Samuel, Observation of PT phase transition in a simple mechanical system, *American Journal of Physics*, vol. 81, no. 3, pp. 173-179, Mar. 2013.
- [19] E. N. Tsoy, Coupled oscillators with parity-time symmetry, *Physics Letters A*, vol. 381, no. 5, pp. 462-466, Feb. 2017.
- [20] X.-W. Xu, Y. Liu, C.-P. Sun, and Y. Li, Mechanical PT-symmetry in coupled optomechanical systems, *Physical Review A*, vol. 92, no. 1, Jul. 2015.
- [21] W. Li, Y. Jiang, C. Li, and H. Song, Parity-time-symmetry enhanced optomechanically-induced-transparency, *Scientific Reports*, vol. 6, no. 1, Aug. 2016.
- [22] L.-Y. He, Parity-time-symmetry-enhanced sideband generation in an optomechanical system, *Physical Review A*, vol. 99, no. 3, Mar. 2019.
- [23] C. Jiang, Y. Cui, Z. Zhai, H. Yu, X. Li, and G. Chen, Tunable slow and fast light in parity-time-symmetric optomechanical systems with phonon pump, *Optics Express*, vol. 26, no. 22, p. 28834, Oct. 2018.
- [24] X. Zhu, H. Ramezani, C. Shi, J. Zhu, and X. Zhang, PT-symmetric acoustics, *Phys. Rev. X* 4, 031042 (2014).
- [25] R. Fleury, D. Sounas, and A. Alu, An invisible acoustic sensor based on parity-time symmetry, *Nat. Commun.* 6, 5905 (2015).
- [26] C. Shi, M. Dubois, Y. Chen, L. Cheng, H. Ramezani, Y. Wang, and X. Zhang, Accessing the exceptional points of parity-time symmetric acoustics, *Nat. Commun.* 7, 11110 (2016).
- [27] J. Schindler, A. Li, M. C. Zheng, F. M. Ellis, and T. Kottos, Experimental study of active LRC circuits with PT-symmetries, *Physical Review A*, vol. 84, no. 4, Oct. 2011.
- [28] J. Schindler, Z. Lin, J. M. Lee, H. Ramezani, F. M. Ellis, and T. Kottos, PT-symmetric electronics, *Journal of Physics A: Mathematical and Theoretical*, vol. 45, no. 44, p. 444029, Oct. 2012.
- [29] F. Fotsa-Ngaffo, S. B. Tabeu, S. Tagouegni, and A. Kenfack-Jiotsa, Thresholdless characterization in space and time reflection symmetry electronic dimers, *Journal of the Optical Society of America B*, vol. 34, no. 3, p. 658, Feb. 2017.
- [30] S. B. Tabeu, F. Fotsa-Ngaffo, and A. Kenfack-Jiotsa, Non-Hermitian Hamiltonian of two-level systems in complex quaternionic space: An introduction in electronics, *EPL (Europhysics Letters)*, vol. 125, no. 2, p. 24002, Feb. 2019.
- [31] S. B. Tabeu, F. Fotsa-Ngaffo, and A. Kenfack-Jiotsa, Imaginary resistor based Parity-Time symmetry electronics dimers, *Optical and Quantum Electronics*, vol. 51, no. 10, p. 335, Oct. 2019.
- [32] X. Wang and J.-H. Wu, Optical PT-symmetry and PT-antisymmetry in coherently driven atomic lattices, *Optics Express*, vol. 24, no. 4, p. 4289, Feb. 2016.
- [33] P. Peng, W. Cao, C. Shen, W. Qu, J. Wen, L. Jiang, and Y. Xiao, Antiparity-time symmetry with flying atoms, *Nature Physics*, vol. 12, no. 12, pp. 1139-1145, Aug. 2016
- [34] C. Zheng, Duality quantum simulation of a generalized anti-PT-symmetric two-level system, *EPL (Europhysics Letters)*, vol. 126, no. 3, p. 30005, Jun. 2019.
- [35] B. Lu, X.-F. Liu, Y.-P. Gao, C. Cao, T.-J. Wang, and C. Wang, Berry phase in an anti-PT symmetric metal-semiconductor complex system, *Optics Express*, vol. 27, no. 16, p. 22237, Jul. 2019.
- [36] Y. Li, Y. Peng, L. Han, M.-A. Miri, W. Li, M. Xiao, X.-F. Zhu, J. Zhao, A. Alù, S. Fan, C.-W. Qiu,

- Anti-parity-time symmetry in diffusive systems *Science* Vol. 364, Issue 6436, pp. 170-17312 Apr 2019:
- [37] J. Zhao, Y. Liu, L. Wu, C.-K. Duan, Y. Liu, and J. Du, Observation of Anti-PT-Symmetry Phase Transition in the Magnon-Cavity-Magnon Coupled System," *Physical Review Applied*, vol. 13, no. 1, Jan. 2020.
- [38] J. Wen, G. Qin, C. Zheng, S. Wei, X. Kong, T. Xin, and G. Long, Observation of information flow in the anti-PT-symmetric system with nuclear spins, *npj Quantum Information*, vol. 6, no. 1, Mar.2020.
- [39] K. Shouno, Y. Ishibashi, Synthesis and active realization of a three-phase complex coefficient filter using gyrators. In: 51st Midwest Symposium on Circuits and Systems IEEE MWSCAS 2008, vol.87, pp. 550-553 (2008)
- [40] S. B. Tabeu, F. Fotsa-Ngaffo, and A. Kenfack-Jiotsa, Observation of Hermitian and Non-Hermitian Diabolic Points and Exceptional Rings in Parity-Time symmetric ZRC and RLC Dimers, arXiv:2005.11311 [physics.app-ph] (2020)
- [41] P.-Y. Chen, M. Sakhdari, M. Hajizadegan, Q. Cui, M. M.-C. Cheng, R. ElGanainy, and A. Alù, Generalized parity-time symmetry condition for enhanced sensor telemetry," *Nature Electronics*, vol.1, no. 5, pp. 297-304, May 2018.
- [42] M. Hajizadegan, M. Sakhdari, S. Liao, and P.-Y. Chen, High-Sensitivity Wireless Displacement Sensing Enabled by PT-Symmetric Telemetry, *IEEE Transactions on Antennas and Propagation*, vol. 67, no. 5, pp. 3445-3449, May 2019.
- [43] L. O'Brien, Optical Quantum Computing, *Science*, vol. 318, no.5856, pp. 1567-1570, Dec. 2007.
- [44] P. Kok, W. J. Munro, K. Nemoto, T. C. Ralph, J. P. Dowling, and G. J. Milburn, Linear optical quantum computing with photonic qubits, *Reviews of Modern Physics*, vol. 79, no. 1, pp. 135-174, Jan. 2007
- [45] M. G. Thompson, A. Politi, J. C. F. Matthews, and J. L. O'Brien, Integrated waveguide circuits for optical quantum computing, *IET Circuits, Devices Systems*, vol. 5, no. 2, p. 94, 2011
- [46] C. Zheng, Duality quantum simulation of a general parity-time-symmetric two-level system, *EPL (Europhysics Letters)*, vol. 123, no. 4, p. 40002, Sep. 2018